Polymorph Discrimination of $CaCO_3$ Mineral in an Ethanol/Water Solution: Formation of Complex Vaterite Superstructures and Aragonite Rods

Shao-Feng Chen,[†,§] Shu-Hong Yu,*[,†,‡,§] Jun Jiang,[†,‡] Fanqing Li,[†] and Yankuan Liu[‡]

Division of Nanomaterials & Chemistry, Hefei National Laboratory for Physical Sciences at Microscale, Structure Research Laboratory of CAS, University of Science and Technology of China, Hefei 230026, People's Republic of China, Department of Chemistry, University of Science and Technology of China, Hefei 230026, People's Republic of China, and Department of Materials Science and Engineering, University of Science and Technology of China, Hefei 230026, People's Republic of China

Received August 23, 2005. Revised Manuscript Received October 31, 2005

Polymorph discrimination of $CaCO_3$ mineral has been easily realized in an ethanol/water mixed solution system under mild conditions without using any organic additives. The phase transition from a mixture of calcite and aragonite to pure aragonite, and then to almost pure vaterite, can be nicely captured by the choice of a suitable ratio of ethanol to distilled water in the present reaction system. In addition, a complex self-assembly process for the formation of multilayered vaterite cakes in this binary solution system has been proposed. The cakelike vaterite crystals with multilayered structures are porous with an average pore size of 24.9 nm. The results demonstrated that such a binary reaction media could provide an alternative and versatile tool for controlling the polymorph and nanostructures of inorganic minerals through manipulating the thermodynamics and kinetics. This study provides an alternative polymorph switching route for $CaCO_3$ mineral without using any additives and can even be scaled up as a green chemistry method for the industrial production of $CaCO_3$ with different polymorphs.

1. Introduction

Calcium carbonate, as one of the most widely existing biominerals produced by organisms, has three anhydrous crystalline phases—calcite, aragonite, and vaterite—and two hydrated ones, including mono- and hexahydrate. From the viewpoint of thermodynamics, calcite is more stable than aragonite, and both are main forms of calcium carbonate existing in organisms.[1−3] Vaterite is the least stable of these three phases and easily transforms into calcite in a chemistry laboratory; however, only a trace amount of vaterite exists in organisms.[4] Although the amount of vaterite is far less than that of calcite and aragonite, it also plays key roles in biological life and health.[5,6]

Many approaches have been widely chosen to control the phases and morphology of calcium carbonate as reviewed by Cölfen.[7] These approaches include microemulsion,[8,9] natural and synthetic matrixes,[10−12] Langmuir monolayers,[13] self-assembled monolayers (SAMs),[14]solvothermal processes,[15] and soft chemistry.[16,17] Double-hydrophilic block copolymers (DHBCs),[18,19] dendrimers,[20] polymers or monomers of amino acids,[21,22] and gelatin[23] have also been recently introduced to control and stabilize the metastable vaterite phase. Furthermore, the adjustment of the pH value and initial supersaturation of solution, molecular weight, and concentration of polymer also exerts some influences on polymorphs of $CaCO_3$.[9,17,24,25] Recently, our group has demonstrated the

* Correspondence should be addressed to this author. Fax: + 86 551 3603040. E-mail: shyu@ustc.edu.cn.
† Structure Research Laboratory of CAS.
‡ Department of Chemistry.
§ Department of Materials Science and Engineering.

(1) Young, J. R.; Davis, S. A.; Bown, P. R.; Mann, S. *J. Struct. Biol.* **1999**, *126*, 195.
(2) Cölfen, H.; Mann, S. *Angew. Chem., Int. Ed.* **2003**, *42*, 2350.
(3) Kato, T.; Sugawara, A.; Hosoda, N. *Adv. Mater.* **2002**, *14*, 869.
(4) Brown, R.; Severin, K. P.*Can. J. Fish. Aquat. Sci.* **1999**, *56*, 1898.
(5) Burt, H. M.; Jackson, J. K.; Taylor, D. R.; Crowther, R. S. *Dig. Dis. Sci.* **1997**, *42*, 1283.
(6) Taylor, D. R.; Crowther, R. S.; Cozart, J. C.; Sharrock, P.; Wu, J.; Soloway, R. D. *J. Hepatol.* **1995**, *22*, 488.
(7) Cölfen, H. *Curr. Opin. Colloid Interface Sci.* **2003**, *8*, 23.
(8) Walsh, D.; Lebeau, B.; Mann, S. *Adv. Mater.* **1999**, *11*, 324.
(9) (a) Li, M.; Mann, S. *Adv. Funct. Mater.* **2002**, *12*, 773. (b) Li, M.; Lebeau, B.; Mann, S. *Adv. Mater.* **2003**, *15*, 2032.
(10) Ajikumar, P. K.; Lakshminarayanan, R.; Valiyaveettil, S. *Cryst. Growth Des.* **2004**, *4*, 331.
(11) Hosoda, N.; Kato, T. *Chem. Mater.* **2001**, *13*, 688.
(12) Falini, G.; Fermani, S.; Gazzano, M.; Ripamonti, A. *Chem.*—Eur. J. **1998**, *4*, 1048.
(13) Loste, E.; Díaz-Martí, E.; Zarbakhsh, A.; Meldrum, F. C. *Langmuir* **2003**, *19*, 2830.
(14) Küther, J.; Seshadri, R.; Knoll, W.; Tremel, W. *J. Mater. Chem.* **1998**, *8*, 641.
(15) Li, Q.; Ding, Y.; Li, F. Q.; Xie, B.; Qian, Y. T. *J. Cryst. Growth* **2002**, *236*, 357.
(16) Lee, I.; Han, S. W.; Lee, S. J.; Choi, H. J.; Kim, K. *Adv. Mater.* **2001**, *13*, 1617.
(17) Tai, C. Y.; Chen, F. B. *AIChE J.* **1998**, *44*, 1790.
(18) Cölfen, H.; Antonietti, M. *Langmuir* **1998**, *14*, 582.
(19) (a) See a review and references therein: Yu, S. H.; Cölfen, H. *J. Mater. Chem.* **2004**, *14*, 2124. (b) Qi, L. M.; Li, J.; Ma, J. M. *Adv. Mater.* **2002**, *14*, 300.
(20) See a review and references therein: Naka, K.*Top. Curr. Chem.* **2003**, *228*, 141.
(21) Kitamura, M. *J. Cryst. Growth* **2002**, *237−239*, 2205.
(22) Manolia, F.; Kanakisa, J.; Malkajb, P.; Dalas, E. *J. Cryst. Growth* **2002**, *236*, 363.
(23) Zhan, J. H.; Lin, H.-P.; Mou, C.-Y. *Adv. Mater.* **2003**, *15*, 621.
(24) Park, H. K.; Lee, I.; Kim, K. *Chem. Commun.* **2004**, *10*, 24.
(25) Lakshminarayanan, R.; Valiyaveettil, S.; Loy, G. L. *Cryst. Growth Des.* **2003**, *3*, 953.

10.1021/cm0519028 CCC: $33.50
Published on Web 12/10/2005

formation of superlong helices by tectonic arrangement of $BaCO_3$ nanocrystals induced by a racemic block copolymer,[26] and a PEG-*b*-hexacyclen macrocycle has been used as a crystal growth modifier for controlled self-assembly of complex and unusual calcite pancakes with multiple stacked and porous layers based on a polymer directed crystallization mechanism.[27] Self-assembly of a layerlike clay−polyelectrolyte structure with an interesting analogy to the biomineral nacre has also been reported.[28] In contrast, the influence of solvent on the mineralization of $CaCO_3$ in the absence of organic additives has rarely been studied and the role that simple alcohols play in the polymorph discrimination of $CaCO_3$ mineral is yet not clear.[29−31]

In this paper, an environmentally friendly route is reported for effective polymorph discrimination of $CaCO_3$ mineral in an ethanol/water mixed solution under mild conditions (90 °C) without using any organic additives like previous reports which employed crown ether to produce vaterite.[30,31] Complex cakelike vaterite crystals with porous, multilayered structures, as well as aragonite rods can be selectively synthesized. It has been demonstrated that the thermodynamic and kinetic regimes, which contribute to the polymorph discrimination of calcium carbonate mineral, can be well manipulated in ethanol/water mixed solution by simply tuning the composition of this binary solution.

2. Experimental Section

2.1. Chemicals. All chemicals are of analytical grade. Urea (M_w = 60.06) and calcium acetate (M_w = 176.19) were purchased from Shanghai Chemical Reagent Company. Ethanol (M_w = 46.07) was purchased from the First Zhengxin Chemical Plant of Shanghai. All reagents were used as received without further purification.

2.2. Synthesis Procedure. The method of glass slices treated as a hydrophilic substrate in reaction has been reported elsewhere.[32] Amorphous glass slices were cleaned and sonicated in ethanol for 5 min, then rinsed with double-distilled water and further treated in H_2SO_4/H_2O_2 (volume ratio is 7:3) at about 90 °C for 2 days, and finally washed with double-distilled water and dried with acetone.

In a typical synthesis of vaterite, 0.220 g of calcium acetate and 0.225 g of urea were dissolved in a 25-mL conical bottle containing 5 mL of double-distilled water under magnetic stirring (pH 8.2), and then 15 mL of absolute ethanol was added to the conical bottle. After complete mixing, several glass slices were put into the conical bottle as substrates; then the plug was covered with a thin film of Vaseline petroleum jelly to ensure that the conical bottle was airtight. Finally, the conical bottle containing the mixed solution was heated at 363 K in an oven for 24 h. To understand the effect of anion in the precursor on the phase selection, calcium nitrate (0.295 g) and calcium chloride (0.139 g) were also chosen as calcium resources at R = 3. The reaction at 120 °C was performed in a Teflon-lined autoclave with a volume of 30 mL.

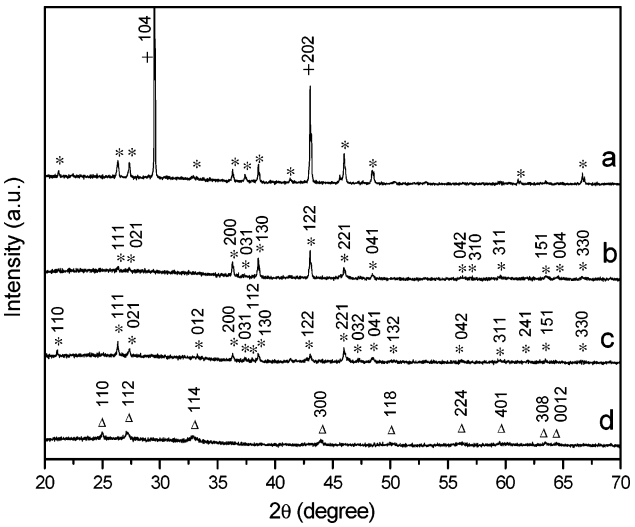

Figure 1. XRD patterns of calcium carbonate obtained after 24 h reaction: (a) R = 0; (b) R = 1/3; (c) R = 1; (d) R = 3. R is the volume ratio of ethanol/water. +, calcite phase (JCPDS Card No. 05-0568); *, aragonite phase (JCPDS Card No. 41-1475); △, vaterite phase (JCPDS Card No. 33-0268).

2.3. Characterization. X-ray powder diffraction (XRD) patterns were carried out on a Philips X'Pert Pro Super Diffractometer with Cu Kα radiation (λ = 1.541 874 Å). Scanning electron microscopic (SEM) images were taken on a JEOL JSM-6700F scanning electron microscope. Fourier transform infrared (FT-IR) spectra were measured on a MAGNA-IR 750 (Nicolet Instrument Co. USA). Transmission electron microscopic (TEM) photographs were taken on a Hitachi Model H-800 transmission electron microscope at an accelerating voltage of 200 kV. Nitrogen sorption data were obtained with a Micromeritics Tristar 3000 automated gas adsorption analyzer. Isotherms were evaluated with the Barrett−Joyner−Halenda (BJH) theory to give the pore parameters, including surface areas, pore size, and pore size distribution.

3. Results and Discussion

3.1. Phase Discrimination in Ethanol−Water Reaction System. The phase transition from a mixture of calcite and aragonite to pure aragonite, and then to almost pure vaterite, can be nicely captured by the choice of a suitable volume ratio of ethanol to distilled water as summarized in Scheme 1.

Scheme 1. Sketch of Relationship between the Mineral Polymorph and the Solvent Composition[a]

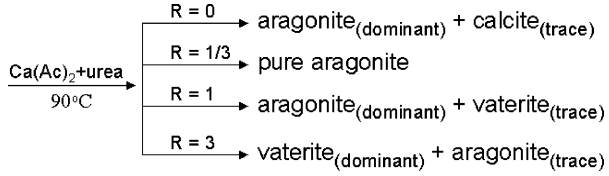

[a] R = volume ratio of ethanol to double-distilled water (v/v).

The X-ray diffraction pattern (XRD) in Figure 1a shows that a mixture of calcite and aragonite was obtained without adding ethanol (R = 0). Two kinds of typical morphologies are observed, as shown in Figure 2. With the increase of the volume ratio of ethanol/water (R = 1/3 and 1, respectively), pure aragonite can be obtained (Figure 1b,c). With a further

(26) Yu, S. H.; Cölfen, H.; Tauer, K.; Antonietti, M. *Nat. Mater.* **2005**, *4*, 51.
(27) Chen, S. F.; Yu, S. H.; Wang, T. X.; Jiang, J.; Cölfen, H.; Hu, B.; Yu, B. *Adv. Mater.* **2005**, *17*, 1461.
(28) Tang, Z. Y.; Kotov, N. A.; Magonov, S.; Ozturk, B. *Nat. Mater.* **2003**, 2, 413.
(29) Dickinson, S. R.; McGrath, K. M. *J. Mater. Chem.* **2003**, *13*, 928.
(30) Doxsee, K. M. *Chem. Mater.* **1998**, *10*, 2610.
(31) Doxsee, K. M.; Saulsbery, R. L. *Materials Science of the Cell*; Mulder, B., Vogel, V., Schmidt, C., Eds.; MRS Symposium Series 489; pp 161−166.
(32) Yu, S. H.; Cölfen, H.; Xu, A. W.; Dong, W. *Cryst. Growth Des.* **2004**, *4*, 33.

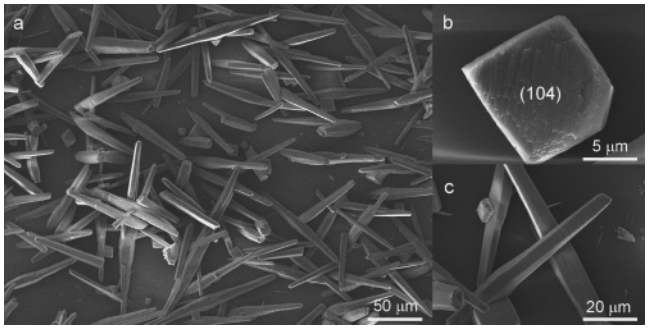

Figure 2. SEM images of sample that contained a majority of aragonite rods and a trace amount of calcite crystals. A 0.220 g sample of calcium acetate and 0.225 g of urea were dissolved in a 25-mL conical bottle containing 20 mL of double-distilled water, $R = 0$, and then kept in an oven at 90 °C. (a) General view of the product with low magnification. (b) Typical calcite crystal. (c) High-magnification image of aragonite rods.

increase of the amount of ethanol to $R = 3$, almost pure vaterite can be obtained (Figure 1d; the number percentage of vaterite crystals is greater than 98%).

However, if the reaction solution with $R = 3$ was vigorously stirred during the reaction, aragonite nanorods became dominant, as shown in Figure 3 (see also Figure 7a). In addition, aragonite nanoribbons, which coexisted with vaterite cakes, were found when the reaction was performed at 120 °C for 24 h ($R = 3$) by a hydrothermal process, as shown in Figure 4 (see also Figure 7b).

Pure aragonite crystals with rodlike shape are obtained through the choice of a suitable volume ratio of $R = 1/3$, as shown in Figure 5a. Rodlike aragonite crystals with a diameter of 4.5 μm and length up to 30 μm are very uniform, and they display a well-defined prismatic shape (Figure 5b). A minority of aragonite crystals with a flower shape are observed, composed of very thin nanorods with a diameter of 30 nm (Figure 5c). With increasing amount of ethanol up to $R = 1$, a scenario of three kinds of morphologies are observed, i.e., dumbbell-like crystals made of aragonite nanorods (dominant), nanorods, and a trace amount of hexagonal plates that may be vaterite phase (Figure 5d−f, the number percentage of hexagonal plates is less than 10%).

The above phase formation was further determined by FT-IR spectroscopy. The samples ($R = 1/3$, 3/17) are pure aragonite phase, which is confirmed by the presence of 700 and 712 cm^{-1} (ν_4 mode), 854 cm^{-1} (ν_2 mode), and 1080 cm^{-1} (ν_1 mode) CO_3^{2-} absorption bands for typical aragonite phase (Figure 6a,b).[33] This is consistent with the result from the XRD pattern shown in Figure 1a. It is worth noting that there exists a trace amount of vaterite at $R = 1$ (Figure 6c), and then vaterite becomes a dominant phase and aragonite is the minor phase at $R = 3$, whose spectrum (Figure 6e) shows the vibrational bands at ca. 744 and 877 cm^{-1} that can be attributed to the ν_4 and ν_2 modes of CO_3^{2-} in vaterite.[34]

However, calcite was a dominant phase if calcium nitrate or calcium chloride was used to substitute for calcium acetate under identical conditions, underscoring the key roles that

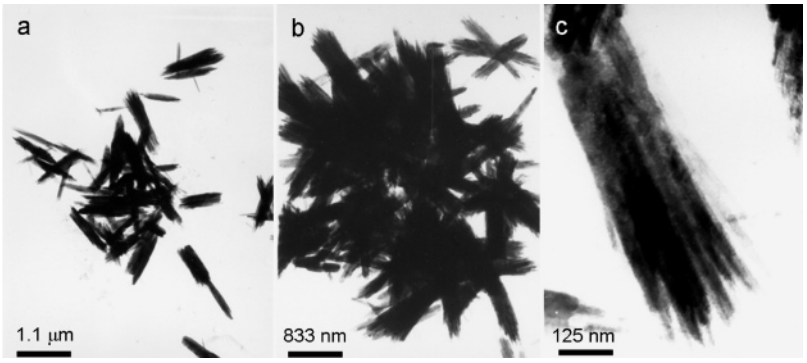

Figure 3. TEM images of sample obtained by a modified synthetic procedure: 0.220 g of calcium acetate and 0.225 g of urea were dissolved in a 25-mL conical bottle containing mixed solvent ($R = 3$) under stirring at 90 °C. (a, b) Low-magnification TEM images; (c) higher magnification TEM image. These bundles are composed of nanorods that are 30−40 nm in width and more than 1 μm in length.

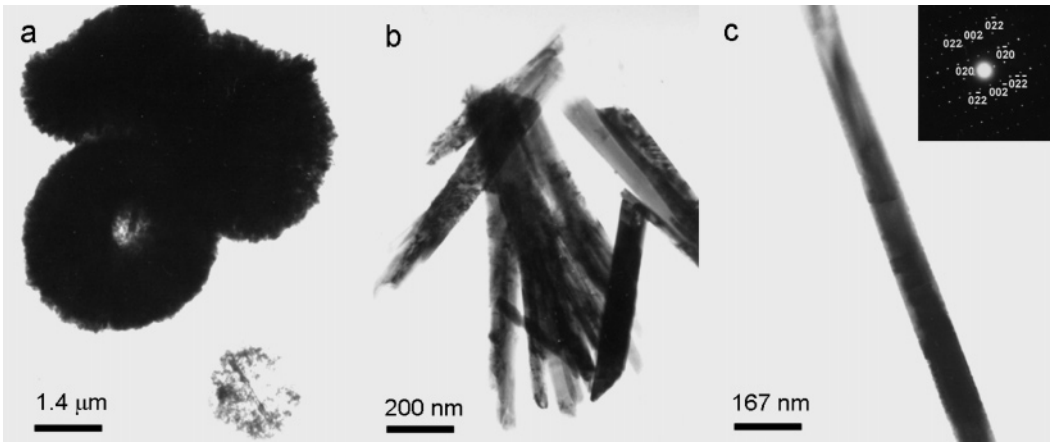

Figure 4. TEM images of sample obtained by hydrothermal method: 0.220 g of calcium acetate and 0.225 g of urea were dissolved in the Teflon-lined stainless steel autoclave containing mixed solvent ($R = 3$) under 120 °C for 24 h. (a) Cakelike vaterite structures. (b) Nanoribbons separated from aggregation by sonication, (c) A single nanoribbon; insert is ED pattern taken along ⟨100⟩.

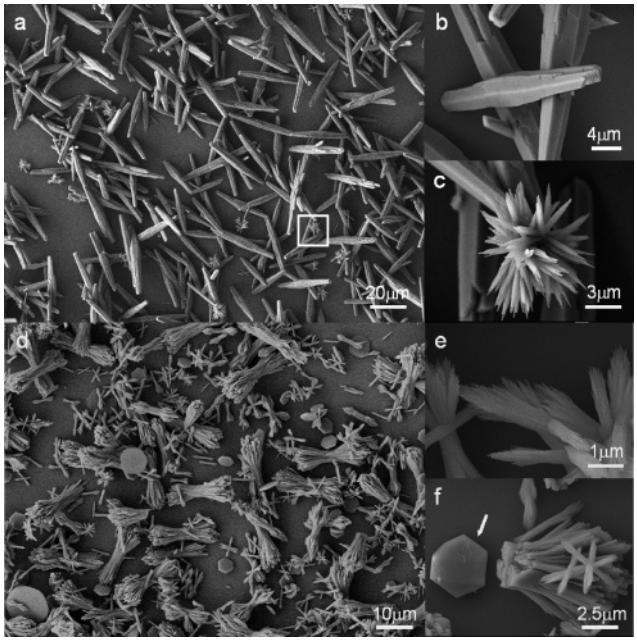

Figure 5. SEM images of calcium carbonate crystal obtained after 24 h reaction. The volume ratio of ethanol to water is (a−c) $R = 1/3$ and (d−f) $R = 1$, respectively. The white arrow indicates the hexagonal plate.

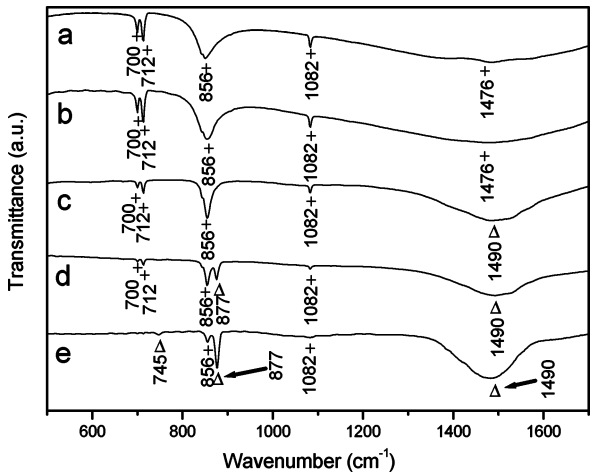

Figure 6. FT-IR spectra of washed calcium carbonate particles: (a) $R = 3/17$, pure aragonite; (b) $R = 1/3$, pure aragonite; (c) $R = 1$, trace amount of vaterite and a majority amount of aragonite; (d) $R = 3/2$, mixture of aragonite and vaterite; (e) $R = 3$, predominantly vaterite and a trace of aragonite. △, Vaterite phase; +, aragonite phase.

the acetate anions played in polymorph discrimination in the present binary solution system (Figure 7).

Previously, Matijevic and co-workers[33] pointed out that aragonite can be generated at low concentration of calcium ion at 90 °C without any organic additives, and Wolf and co-workers[35] reported that the Gibbs energy of transition from vaterite to calcite is about -3 kJ·mol^{-1} when the solvent is pure water. Another document[36] showed that calculated lattice energies of the three polymorphs are very close to each other: the values for calcite, aragonite, and vaterite are

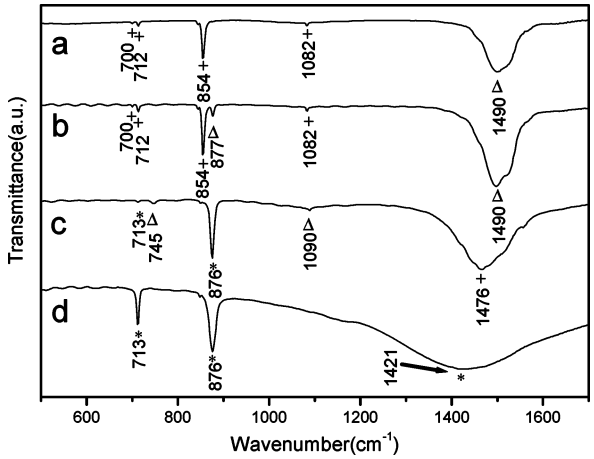

Figure 7. FT-IR spectra of controlled experiments: (a) 0.220 g of calcium acetate and 0.225 g of urea were dissolved in a 25-mL conical bottle containing mixed solvent ($R = 3$) under stirring in 90 °C; (b) 0.220 g of calcium acetate and 0.225 g of urea were dissolved in mixed solvent ($R = 3$) and poured into in a Teflon-lined stainless steel autoclave for hydrothermal reaction at 120 °C for 24 h; (c) 0.295 g of $Ca(NO_3)_2{\cdot}4H_2O$ and 0.225 g of urea were dissolved in a 25-mL conical bottle containing mixed solvent ($R = 3$) and then kept in an oven at 90 °C; (d) 0.139 g of $CaCl_2$ and 0.225 g of urea were dissolved in a 25-mL conical bottle containing mixed solvent ($R = 3$) and then kept in an oven at 90 °C. *, Calcite phase; △, vaterite phase; +, aragonite phase.

-1.6867×10^8, -1.7851×10^8, and -1.6577×10^8 kJ·mol^{-3}, respectively.

According to Gibbs theory,[37] the energy of a crystal is comprised of surface energy and bulk lattice energy. Therefore, the surface energies for these three polymorphs should play a key role in the total energy of a crystal, which is directly related to the difference in solvent properties. This may be the real reason that the three polymorphs can be selectively controlled by altering the value of R or the anion in calcium sources. It is necessary to consider the interaction between ethanol and Ca^{2+} (or O^{2-} of CO_3^{2-}) in the ethanol/water system for the calculation of surface energies. Because the most bared crystal faces of calcite and aragonite are terminated with different atoms,[36] it is reasonable to understand that the extent of decreasing surface energies on calcite and aragonite is not equal by altering the composition of a solvent. Hence, calcite disappears completely but aragonite is stable under these conditions ($R \geq 1/3$), although the accurate bond interaction between $CaCO_3$ and mixed solvent is still not clear.

When the volume of ethanol increases again ($R = 3$), the solvent effect becomes more obvious. It is believed that ethanol around Ca^{2+} ions would form "solvent cages"[38] to shield Ca^{2+} on CO_3^{2-}, which can reduce the activity of CO_3^{2-} during the reaction. In this experiment ($R = 3$), the size of building blocks for the obtained vaterite superstructures is less than 10 nm. Although the thermodynamics of calcium carbonate on nanoscale is not well understood yet, we can conclude that the higher ratio of surface atoms to bulk atoms than that in a macroscopic system can lead to a significant increase in surface energy because the weight of surface energy is increased in the total energies of the crystals when

(33) Wang, L. F.; Sondi, I.; Matijevic, E. *J. Colloid Interface Sci.* **1999**, *218*, 545.
(34) White, W. B. In *Infrared Spectra of Mineral*; Farmer, V. C., Ed.; Mineralogical Society: London, 1974; pp 227−284.
(35) Wolf, G.; Konigsberger, E.; Schmidt, H. G.; Konigsberger, L. C.; Gamsjager, H. *J. Therm. Anal.* **2000**, *60*, 463.
(36) de Leeuw, N. H.; Parker, S. C. *J. Phys. Chem. B* **1998**, *102*, 2914.
(37) Gibbs, J. W. In *Collected Works*; Longman: New York, 1928.
(38) Dedonder-Lardeux, C.; Gregoire, G.; Jouvet, C.; Martrenchard, S.; Solgadi, D. *Chem. Rev.* **2000**, *100*, 4023.

the crystals are small as reported by Gibbs,[37] which may favor the formation of vaterite in such a complex local environment.[31] Furthermore, increasing the ethanol content in the solvent mixture decreases the solubility of $CaCO_3$, thus increasing the tendency of supersaturation which favors faster precipitation of the kinetic phase, i.e., vaterite phase from the viewpoint of kinetics as reported by Xyla et al.[39] The results demonstrate that phase switching can be achieved by changing the ratio of thermodynamic and kinetic control.

By contrast, if the reaction temperature was increased to 120 °C for hydrothermal reaction or this reaction was performed under stirring at 90 °C ($R = 3$), aragonite became a dominant phase (Figure 7a,b). These results stated above implied that polymorph discrimination of aragonite and vaterite (90 °C, $R = 3$, without stirring) can be regarded as mainly under thermodynamic control by aggrandizing the weight of surface energy in the total energy. Thus, the phenomenon stated above—disappearance of calcite and appearance of metastable vaterite—may benefit from decreasing the differences in surface energy for different polymorphs of calcium carbonate due to the presence of ethanol. This is similar to what has been found in the phase transition of $CeOHCO_3$ in an ethanol/water solution as we reported previously.[40] Actually, harvesting an absolutely pure metastable phase (here, vaterite) is difficult even though the pH value and concentration of urea are controlled as reported previously.[17] This phenomenon could be due to the following reasons: (i) the Gibbs free energy of phase transition between the metastable phase and the stable phase is rather low; (ii) the vaterite product is usually composed of nanocrystals and thus has a high surface area in addition to the instability of the vaterite phase, so dissolution and recrystallization to other more stable phases become possible; and (iii) the kinetics in mixed solvent solution are too complex to be controlled precisely.

3.2. Complex Cakelike Vaterite Crystals with Porous and Multilayered Structures. Field-emission SEM images of vaterite crystals grown at $R = 3$ show multilayered cakes with rather rough surfaces (Figure 8). There exists a majority of cakelike crystals and only a few dumbbell-like crystals; the diameter and thickness of crystals are about 2−4 μm and 0.8−1.5 μm, respectively (Figure 8a). It is interesting that the middle section of the crystals is sunken and that the thickness of each layer of the cake is about 50−100 nm (Figure 8b). Nevertheless, the presence of dumbbell-like crystals hints that this sample is still not absolutely pure vaterite, which can also be auxiliarily detected by FT-IR spectroscopy (Figure 6e). Examination of the early-stage sample shows that the cakes have already been produced after reaction for 6 h (Figure 8c,d). Each also has the multilayered structure similar to that shown in Figure 8b; however, the surfaces of the cakes obtained in the early stage are rougher than those of the ripened cakes.

To understand the formation process of such multilayered cakes, the time-dependent shape evolution process was

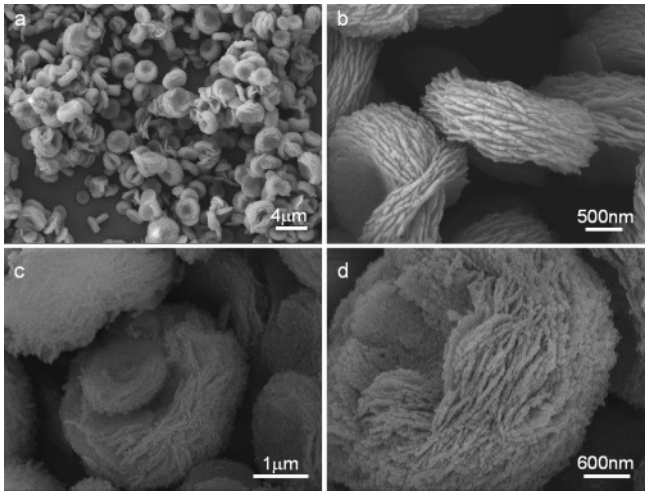

Figure 8. (a) SEM image of vaterites obtained after reaction at 90 °C for 24 h. $R = 3$. (b) High-magnification SEM image of vaterite cakes with multilayers. (c) SEM image of vaterites obtained after reaction at 90 °C for 6 h. $R = 3$. (d) High-magnification SEM image of (c).

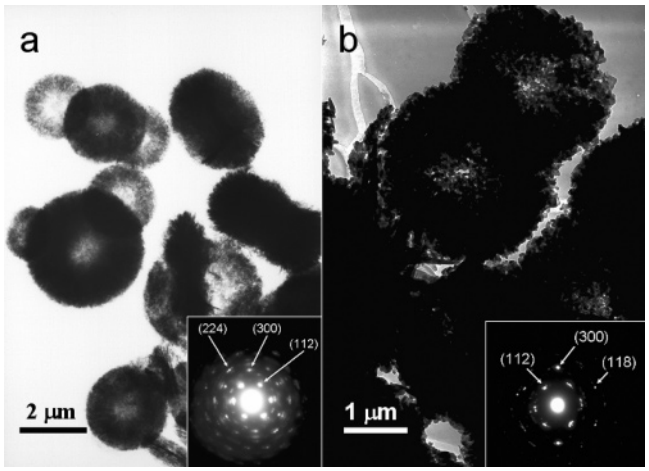

Figure 9. Typical images of transmission electron microscopy (TEM) of the sample ($R = 3$) obtained after reaction for different times: (a) 6 and (b) 24 h. Insert is the electron diffraction pattern.

followed by careful examination of the intermediates. The central parts of the cakes obtained after 6 h are looser than the edges of such crystals (Figures 8c,d); even more, some crystals are "hollow" in the center and look like rings, as observed by TEM as shown in Figure 9a. The electron diffraction pattern indicates that these products are polycrystalline (insert in Figure 9a) and are formed by the aggregation of many tiny nanoparticles. We cannot have this sample (obtained after reaction for 6 h) tested by high-resolution TEM because the structure will rapidly "melt" upon exposure to an electron beam. In fact, we cannot have even pictures of higher magnification than that of shown in Figure 9a, and this phenomenon provides direct evidence to show how small the building blocks are. With prolonged time, the "hollow" cakes became much fuller after reaction for 24 h, and the electron diffraction pattern shows that the structure is polycrystalline vaterite phase, too (Figure 9b). We find that the diameter of cakes collected after reaction for 6 h is close to that of the product obtained after 24 h, suggesting that the crystals are growing with prolonged time, but accompanying a restructuring process and self-assembly along the thickness direction of the cake.

(39) Xyla, A. G.; Giannimaras, E. K.; Koutsoukos, P. G. *Colloids Surf.* **1991**, *53*, 241.
(40) Chen, S. F.; Yu, S. H.; Yu, B.; Ren, L.; Yao, W. T.; Cölfen, H. *Chem.*—Eur. J. **2004**, *10*, 3050.

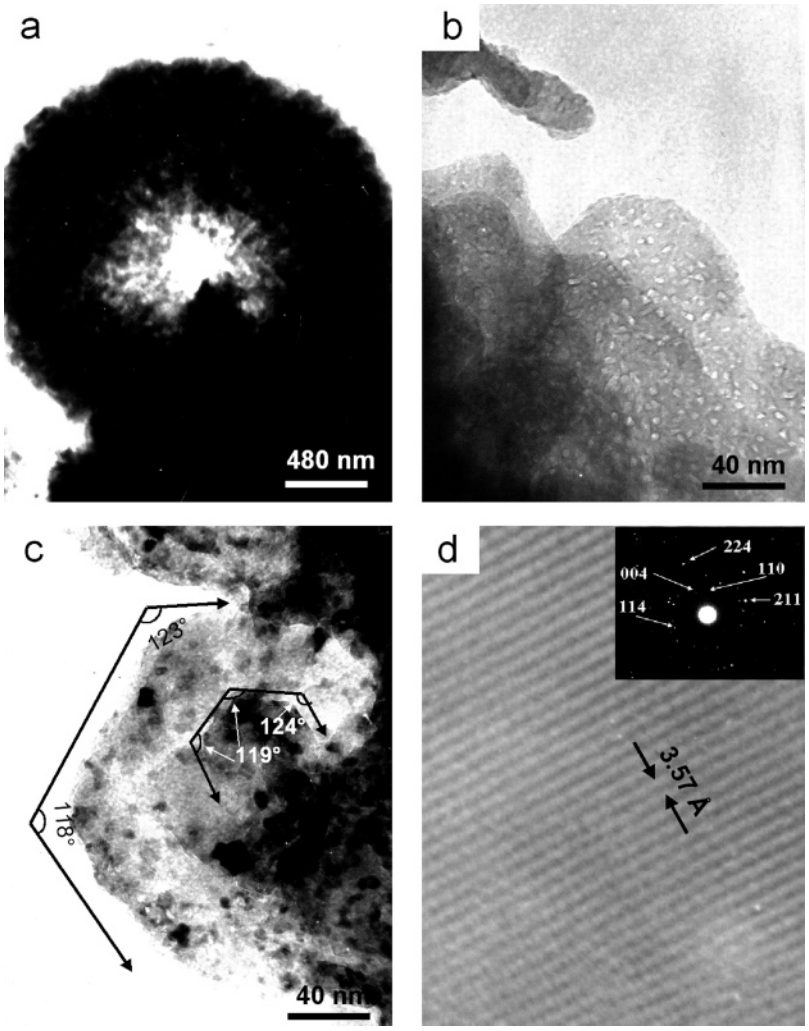

Figure 10. (a) TEM image of vaterite obtained after reaction at 90 °C for 24 h. $R = 3$. (b, c) TEM images of the edge of crystal shown in (a). (d) HRTEM image of the structure shown in (c); the insert is the select area electron diffraction pattern (SAED).

More information can be further provided by high-resolution TEM images of the vaterite obtained after 24 h (Figure 10). Clearly, the structure is multilayered by self-stacking (Figure 10b,c). Moreover, a large number of mesopores with diameters from 2 to 10 nm (Figure 10b) are observed, indicating that this vaterite structure is porous to some extent. From Figure 10c, two pieces of quasi-hexagonal plates can be identified at the bottom of the edge of the structure shown in Figure 10a, in which the angles of adjacent edges are close to 120°, corresponding to the habit of hexagonal symmetry. The selected area diffraction pattern (inserted in Figure 10d) on the edge of a cake indicates that it is polycrystalline vaterite, and the value of the lattice spacings of 3.57 Å measured in the high-resolution TEM image (Figure 9d) is consistent with that for the (110) interplane spacing of vaterite. Figure 11 shows a typical high-resolution TEM (HRTEM) image taken on a large area suggests that the integrated lattice line is composed of two lattice spacings of 3.57 and 3.29 Å, corresponding to those of the (110) and (112) planes.

In the present case, the multilayered cakelike particles are quite different from those lenslike single crystals obtained by a room-temperature gas-diffusion crystallization technique.[41] However, the stacking way of the cakes here is quite similar to that of the lenslike single crystals. It has been reported that [001] oriented vaterite nanosheets presumably stabilized by ammonium are stacked to hexagonal superplates with subsequent fusion to a single crystal by three-dimensional oriented attachment, which could be described by a mesoscale assembly process.[41] From the HRTEM image in Figure 11, the randomly organized vaterite particles within a layer can be explained by an aggregation and recrystallization mechanism; those particles will integrate into polycrystalline layers under control of the Ostwald ripening process.

Since the solvent boiling point of this composition ($R =$ 3) is slightly lower than 90 °C, it is reasonable to believe that plenty of bubbles, which could be composed of NH_3, CO_2, and evaporant of ethanol/water, resided in the solution under boiling conditions. Previously, it has been reported that the interface of liquid−gas can be used to template calcium carbonate superstructures by combination of a surfactant/polymer with an external template such as CO_2 bubbles, for example, either in a microemulsion system[8] or under control of a double-hydrophilic block copolymer.[42] In

(41) Gehrke, N.; Colfen, H.; Pinna, N.; Antonietti, M.; Nassif, N. *Cryst. Growth Des.* **2005**, *5*, 1317.

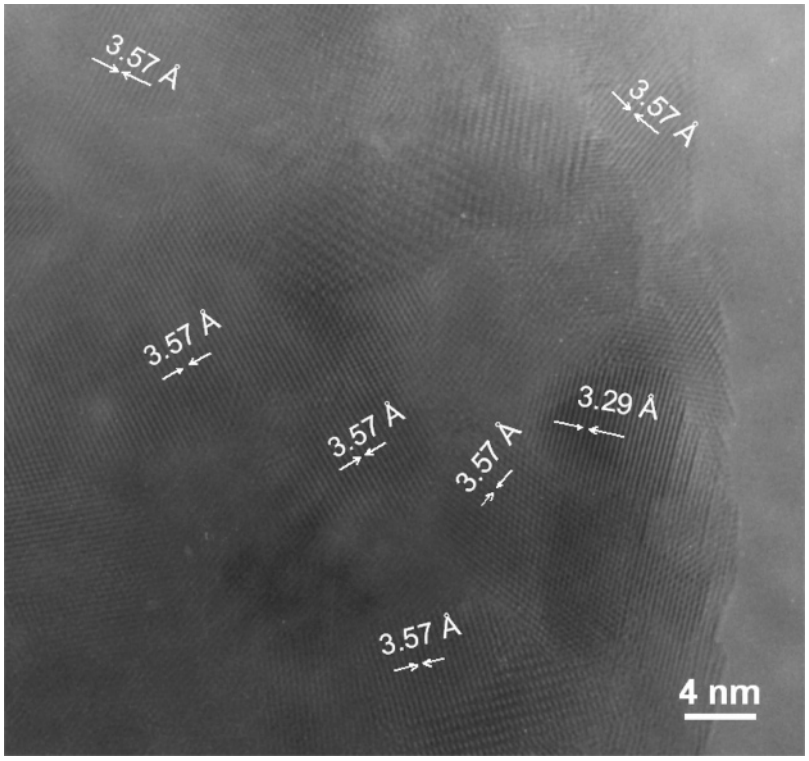

Figure 11. High-resolution TEM image of a part of Figure 10c. The lattice spacings of 3.57 and 3.29 Å correspond to the interplane spacings of (110) and (112) faces of vaterite, respectively.

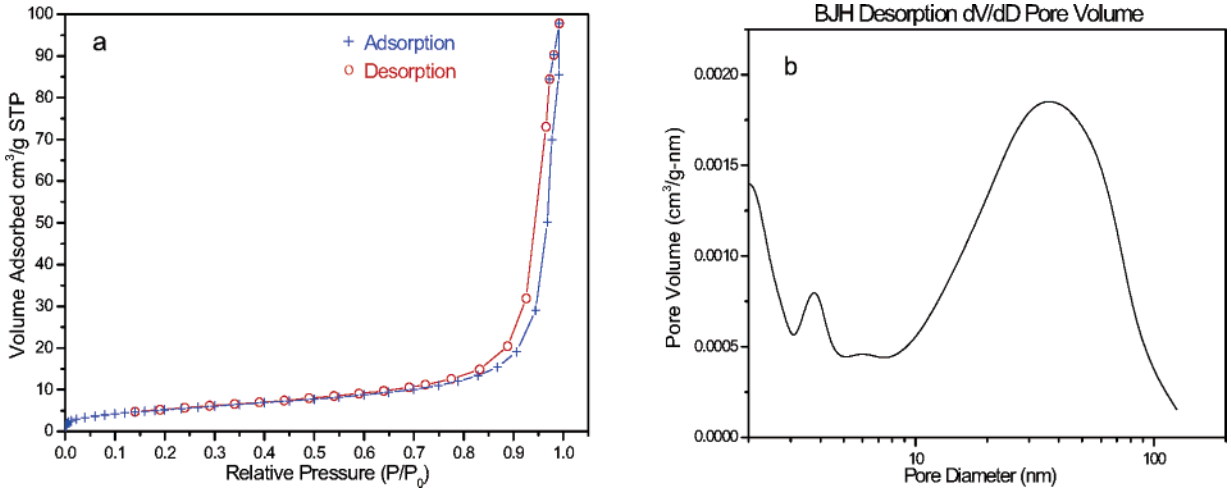

Figure 12. (a) Typical N_2 gas adsorption−desorption isotherm of mesoporous structures of $CaCO_3$. (b) Calculated corresponding size distribution of the mesopores.

the present case, we believe that the formation of mesopores and a hollow area in the central part of the cakes may be relevant to the quasi-stable existence of bubbles.

This assumption could be further supported by the following two designed experiments. A similar reaction at 90 °C at $R = 3$ was done under vigorously stirring and indicated that the stable and statically existing bubbles were completely destroyed, resulting in no cakelike superstructures being found (Figure 3). In another experiment, carbon dioxide gas was bubbled into the solution for several hours before the reaction. The results show that the cakelike structures were still preserved but the inside and outside diameters of the hollow cakes became larger, indicating that the gas−liquid interfaces indeed have influence on the structural formation.

Furthermore, the nitrogen adsorption−desorption isotherm of the mesoporous structures (shown in Figure 7) of $CaCO_3$ was investigated (Figure 12). The Brunauer−Emmett−Teller (BET) surface area is 19.60 m^2/g, and the Barrett−Joyner−Halenda (BJH) adsorption/desorption average pore diameter is 27.9/24.9 nm. It is noticed that the sizes of mesopores centralize on two areas: the peak values are 4 and 30 nm, respectively, in the BJH desorption curve, corresponding to the blank middle section and mesopores in the edge areas of layers (Figure 10b,c).

On the basis of the above analysis, the formation mechanism of these cakes was proposed as illustrated in Scheme

(42) Rudloff, J.; Cölfen, H. *Langmuir* **2004**, *20*, 991.

Scheme 2. Schematic Illustration of the Growth of Cakelike Vaterite Crystals

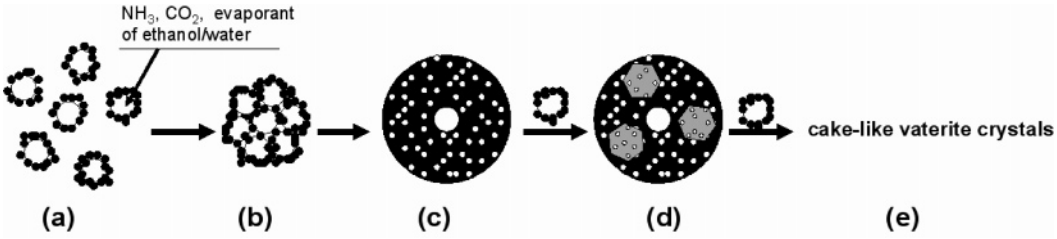

2. A mass of quasi-stable bubbles formed firstly in the solution while primary nanoparticles formed at the liquid−gas interface of bubbles (Scheme 2a). Subsequently, just as Scheme 2b shows, these particulates around bubbles were pushed away from the central area under the influence of surface tension and gravitation after the formation of bubble clusters and bigger bubbles owing to their collision and aggregation. Then, the primary nanoparticles joined by aggregation and recrystallization to become larger, and then integrated into polycrystalline layers under control of the Ostwald ripening process, leaving the contours of bubbles (mesopores and the blank middle section) in some local regions (see Scheme 2c). Finally, many other bubbles with primary nanoparticles were attracted on the formed layers to produce new layers in a stacking way[41] (see Figure 10b,c and Scheme 2d) or to fill in the blank central area probably because the {110} faces of vaterite have relatively larger surface and attachment energies.[36] Repeating the above processes could result in thickening of the edges of the structures and a stagnating growth in the middle section of the cake. Therefore, thickness of the edge of cakes is always larger than that of the middle section and some products even look like rings. It must be pointed out that the real mechanism is rather complicated and needs more dedicated work in the future.

4. Conclusion

In summary, we demonstrated a new route for polymorph discrimination of $CaCO_3$ mineral in an ethanol/water mixed solution system under mild conditions without using any organic additives. The phase transition from a mixture of calcite and aragonite to pure aragonite, and then to almost pure vaterite, can be nicely captured by the choice of a suitable ratio of ethanol to distilled water in the present reaction system. The cakelike vaterite crystals are composed of stacked multilayers, which are porous nanostructures with an average pore diameter of 24.9 nm. A mechanism about nanoparticles self-assembled around gaseous bubbles to form multilayered cakes was proposed. The results have demonstrated that the thermodynamic and kinetic regimes, which contribute to the polymorph discrimination of calcium carbonate mineral, can be well manipulated in the ethanol−water system by simply adjusting the composition of this binary solution. Furthermore, the present study provides an alternative and polymorph switching method for $CaCO_3$ mineral without the use of any organic additives, which can be scaled up as a green chemistry method for the industrial production of $CaCO_3$ with different polymorphs. Such binary reaction media could provide an alternative and versatile tool for controlling the polymorphs and nanostructures of inorganic minerals.

Acknowledgment. S.-H.Y. thanks the special funding support from the Century Program of Chinese Academy of Sciences and the National Science Foundation of China (NSFC), the Distinguished Team of NSFC (Grants 20325104, 20321101, 50372065), the Scientific Research Foundation for the Returned Overseas Chinese Scholars, the Specialized Research Fund for the Doctoral Program (SRFDP) of Higher Education, and the State Education Ministry. This work is partially supported by the Partner-Group of Max Planck Society−Chinese Academy of Sciences. We also thank the referees of this paper for their valuable comments during the revision stage of our manuscript.

CM0519028